THE JOURNAL OF BIOLOGICAL CHEMISTRY VOL. 284, NO. 46, pp. 32040–32052, November 13, 2009

Activating Mutations of the TRPML1 Channel Revealed by Proline-scanning Mutagenesis*[S]

Received for publication, June 24, 2009 Published, JBC Papers in Press, July 28, 2009, DOI 10.1074/jbc.M109.037184

Xian-ping Dong[‡1], Xiang Wang[‡1], Dongbiao Shen[‡1], Su Chen[‡], Meiling Liu[‡], Yanbin Wang[‡], Eric Mills[‡], Xiping Cheng[‡], Markus Delling[§], and Haoxing Xu[‡2]

From the [‡]Department of Molecular, Cellular, and Developmental Biology, University of Michigan, Ann Arbor, Michigan 48109 and the [§]Department of Cardiology, Children's Hospital Boston, Boston, Massachusetts 02115

The mucolipin TRP (TRPML) proteins are a family of endolysosomal cation channels with genetically established importance in humans and rodent. Mutations of human *TRPML1* cause type IV mucolipidosis, a devastating pediatric neurodegenerative disease. Our recent electrophysiological studies revealed that, although a TRPML1-mediated current can only be recorded in late endosome and lysosome (LEL) using the lysosome patch clamp technique, a proline substitution in TRPML1 (TRPML1^{V432P}) results in a large whole cell current. Thus, it remains unknown whether the large TRPML1^{V432P}-mediated current results from an increased surface expression (trafficking), elevated channel activity (gating), or both. Here we performed systemic Pro substitutions in a region previously implicated in the gating of various 6 transmembrane cation channels. We found that several Pro substitutions displayed gain-of-function (GOF) constitutive activities at both the plasma membrane (PM) and endolysosomal membranes. Although wild-type TRPML1 and non-GOF Pro substitutions localized exclusively in LEL and were barely detectable in the PM, the GOF mutations with high constitutive activities were not restricted to LEL compartments, and most significantly, exhibited significant surface expression. Because lysosomal exocytosis is Ca^{2+}-dependent, constitutive Ca^{2+} permeability due to Pro substitutions may have resulted in stimulus-independent intralysosomal Ca^{2+} release, hence the surface expression and whole cell current of TRPML1. Indeed, surface staining of lysosome-associated membrane protein-1 (Lamp-1) was dramatically increased in cells expressing GOF TRPML1 channels. We conclude that TRPML1 is an inwardly rectifying, proton-impermeable, Ca^{2+} and Fe^{2+}/Mn^{2+} dually permeable cation channel that may be gated by unidentified cellular mechanisms through a conformational change in the cytoplasmic face of the transmembrane 5 (TM5). Furthermore, activation of TRPML1 in LEL may lead to the appearance of TRPML1 proteins at the PM.

TRPML1, TRPML2, and TRPML3 are members of the mucolipin family of transient receptor potential (TRPML)[3] proteins believed to encode ion channels of intracellular endosomes and lysosomes (1–7). Recently, the physiological importance of TRPML channels was established genetically. Mutations of human *TRPML1* cause type IV mucolipidosis, a devastating neurodegenerative disease in young children (8–10). Patients with type IV mucolipidosis exhibit motor defects, mental retardation, retinal degeneration, and iron-deficiency anemia (7, 11–13). Mice with mutations in *TRPML3* (*varitint-waddler*, *Va* mice) are deaf and have vestibular and pigmentation defects (14–19). Mutations in *TRPML* in *Caenorhabditis elegans* and *Drosophila* also result in type IV mucolipidosis-like phenotypes at the cellular and/or animal levels (20, 21). The broad spectrum phenotypes of both type IV mucolipidosis and *Va* appear to result from certain aspects of endolysosomal dysfunction (7). Lysosomes, traditionally believed to be the terminal "recycling centers" for biological "garbage," were recently found to play indispensable roles in multiple intracellular signaling pathways (22, 23). The one or more putative endolysosomal functions of TRPML proteins, however, remain unclear, largely due to the lack of a reliable functional assay for these intracellularly localized proteins.

A spontaneous mutation in mouse TRPML3 has shed some light on the physiological functions of TRPML channels. This alanine-to-proline mutation in TRPML3 at the cytoplasmic face of the predicted TM5 (TRPML3^{A419P}or TRPML3^{Va}) causes the vestibular and pigmentation defects of the *Va* phenotypes. Recently, four groups concurrently and independently reported that the *Va* mutation dramatically increases the whole cell current of cells expressing TRPML3 (16–19). Although the current mediated by wild-type (wt) TRPML3 (I_{TRPML3}) is relatively small and can be potentiated by extracellular Na^+ manipulation (removal followed by re-addition), $I_{TRPML3\text{-}Va}$ is large and cannot be further activated by Na^+ manipulation (17, 24). Thus, TRPML3^{Va} is referred to as a gain-of-function (GOF) mutation (25). Furthermore, because Pro introduction into a transmembrane α-helix often causes kinks, hinges, or swivels (26), the "helix-breaking effect" of Pro was proposed to lock the TRPML3^{Va} channel in an unregulated and "open" state (25). Moreover, a Pro scan of the whole TM5 of TRPML3 revealed multiple additional GOF Pro substitutions (16). It is not known

* This work was supported, in whole or in part, by National Institutes of Health Grant NS062792 (to H. X.). This work was also supported by startup funds (to H. X.) from the Department of Molecular, Cellular, and Developmental Biology and Biological Science Scholar Program, University of Michigan, and by a pilot grant (to H. X.) from the University of Michigan Initiative on Rare Disease Research.
[S] The on-line version of this article (available at http://www.jbc.org) contains supplemental Table 1.
[1] These authors contributed equally to this work.
[2] To whom correspondence should be addressed: E-mail: haoxingx@umich.edu.
[3] The abbreviations used are: TRPML, mucolipin family of transient receptor potential; wt, wild type; GOF, gain-of-function; TM, transmembrane; PM, plasma membrane; LEL, late endosome and lysosome; GFP, green fluorescent protein; EGFP, enhanced GFP; MES, 4-morpholineethanesulfonic acid; NMDG, *N*-methyl-D-glutamine; pF, picofarad; Lamp-1, lysosome-associated membrane protein-1.

whether these additional GOF mutations behave identically or similarly to TRPML3^{Va}.

The subcellular localization and electrophysiological functions of TRPML1 appear to differ significantly from those of TRPML3. Although a significant portion of overexpressed TRPML3 localizes at the plasma membrane (PM), TRPML1 almost exclusively localizes in the late endosome and lysosome (LEL) (4, 16–19, 27). Consistent with this, TRPML3 but not TRPML1 displays a significant whole cell current (18). The channel biophysical properties of TRPML1, however, remain controversial. TRPML1 has been reported to be an outwardly rectifying current (28–31), a proton-permeable channel (32, 33), or an NAADP-activated Cs^+-permeable channel with a linear I-V (34, 35). Disagreement also exists as to whether I_{TRPML1} is inhibited (28, 30) or potentiated (18) by protons.

Pro substitution into TRPML1 at the comparable position of the *Va* locus of TRPML3 was shown to display a strong inwardly rectifying proton-impermeable cationic whole cell current that is potentiated by low pH (18). Although TRPML1^{Va} has been successfully used to extrapolate the functions of TRPML1 in LEL (27), it is possible that some channel properties of TRPML1^{Va} may not reflect those of wt TRPML1 *per se*. The *Va* mutation might alter both the gating and pore properties of the TRPML channel (19, 24, 25). Nevertheless, I_{TRPML1} recorded in LEL (lysosomal I_{TRPML1}) is reportedly inwardly rectifying (27), consistent with the I-V of whole cell $I_{TRPML1\text{-}Va}$.

Understanding the mechanisms of the *Va*-induced large whole cell current of TRPML1 may provide insight into the gating and/or trafficking mechanisms of TRPML1. TRPML1 proteins reportedly traffic to the PM via Ca^{2+}-dependent lysosomal exocytosis (36). One of the major sources of Ca^{2+} is from the lysosome itself (22). As a Ca^{2+}-permeable channel, TRPML1 activation may lead to lysosomal exocytosis, hence the surface expression of the channel. Therefore, the effects of the *Va* mutation may result from increased surface expression ("trafficking"), elevated or constitutive channel activity ("gating"), or both. In this study, we obtained several additional GOF *Va*-like mutations and related the channel activities of these mutants to their subcellular localizations and surface (PM) expression.

MATERIALS AND METHODS

Molecular Biology and Histocytochemistry—Full-length mouse TRPML1 was cloned into the EGFP-C2 vector (Clontech) or mCherry as described previously (18, 27). Proline mutations were constructed using a site-directed mutagenesis kit (Qiagen). All constructs were confirmed by sequencing analysis, and protein expression was verified by Western blotting. HEK293T cells were transiently transfected with wt TRPML1 or Pro-substituted TRPML1channels for electrophysiology, confocal imaging, and Mn^{2+} quenching assays. Confocal images were taken using a Leica (TCS SP5) microscope. The Lamp-1 antibody was from the Iowa Hybridoma Bank. The surface expression of Lamp-1 was detected using a mouse monoclonal antibody (H4A3) against the luminal epitope of human Lamp-1 on non-permeabilized cells (37).

Immunodetection of TRPML1 Surface Expression—Cell surface proteins were isolated by using Piece Cell Surface Protein Isolation Kit with some modifications. In brief, HEK293T cells were cultured in polylysine-coated 10-cm dishes and transfected with Pro mutations using Lipofectamine (Invitrogen). After 18 h, cells were washed twice in ice-cold phosphate-buffered saline (pH 8.0) and then incubated with 0.5 mg/ml EZ-Link sulfo-NHS-SS-Biotin (Pierce) in phosphate-buffered saline for 30 min at 4 °C. After 30 min, cells were washed with phosphate-buffered saline (3×), quenched with 500 μl of Quenching Solution (Pierce), and rinsed with Tris-buffered saline (3×). Cells were lysed and sonicated in 500 μl of radioimmune precipitation assay buffer (50 mM Tris, 150 mM NaCl, 1% Triton X-100, 1% Nonidet P-40, 0.5% sodium deoxycholate, 0.1% SDS, 1× protease inhibitor mixture (Roche Applied Science)). Cell lysates were then centrifuged at 10,000 × *g* for 5 min in 4 °C. Supernatant was added to 200 μl of 50% slurry of Neutravidin™-agarose (Pierce) and incubated for 1 h at room temperature. This mixture was washed three times in radioimmune precipitation assay buffer. The proteins were eluted from the Neutravidin™-agarose by heating at 95 °C for 5 min in 2× SDS-PAGE sample buffer. TRPML1 proteins were detected by Western blotting with the anti-GFP antibody 1:5000 (Covance).

Mammalian Cell Electrophysiology—Recordings were performed in transiently transfected HEK293T cells as described previously (18, 27). Cells were cultured at 37 °C, transfected using Lipofectamine 2000 (Invitrogen), and plated onto glass coverslips. The pipette solution contained 147 mM Cs^+, 120 mM methane sulfonate, 4 mM NaCl, 10 mM EGTA, 2 mM Na_2-ATP, 2 mM $MgCl_2$, 20 mM HEPES (pH 7.2, free $[Ca^{2+}]_i < 10$ nM). The standard extracellular bath solution (modified Tyrode solution) contained 153 mM NaCl, 5 mM KCl, 2 mM $CaCl_2$, 1 mM $MgCl_2$, 20 mM HEPES, 10 mM glucose (pH 7.4). The low pH Tyrode solution contained 150 mM sodium gluconate, 5 mM KCl, 2 mM $CaCl_2$, 1 mM $MgCl_2$, 10 mM glucose, 10 mM HEPES, and 10 mM MES (pH 4.6). The low pH $NMDG^+$ solution contained 150 mM NMDG, 10 mM glucose, 10 mM MES, 10 HEPES, with the pH adjusted to 4.6 using methanesulfonic acid. The Zero Divalent solutions contained 10 mM glucose, 20 mM HEPES, 160 mM NaCl, 5 mM KCl (pH 7.4, free $Ca^{2+} < 1$–10 μM). All solutions were applied via a perfusion system that achieved complete solution exchange within a few seconds.

Data were collected using an Axopatch 2A patch clamp amplifier, Digidata 1440, and pClamp 10.0 software (Axon Instruments). Whole cell currents were digitized at 10 kHz and filtered at 2 kHz. The capacity current was reduced as much as possible using the amplifier circuitry. Series resistance compensation was 60–85%. All experiments were conducted at room temperature (~21–23 °C), and all recordings were analyzed with pCLAMP10 (Axon Instruments, Union City, CA) and Origin 7.5 (OriginLab, Northampton, MA).

Endolysosomal Electrophysiology—Endolysosomal patch clamping experiments were performed as described previously (27). Briefly, HEK293T cells were transfected with either EGFP-TRPML1 alone, or cotransfected with mCherry-TRPML1 and EGFP-Lamp-1 (a marker for LEL). Cells were treated with 1–2 μM vacuolin-1 (for 1–2 h) to increase the sizes of the endosomes and lysosomes (38). Vacuoles positive for EGFP-Lamp-1 are


A
mTRPML1 IATLRVALPSVMRFCCCVAVIYLGYCFCGW 444
mTRPML2 ILTMQASLPKVLRFCACAGMIYLGYTFCGW 436
mTRPML3 ILTLQAALPNVMRFCCCAAMIYLGYCFCGW 431
TM5

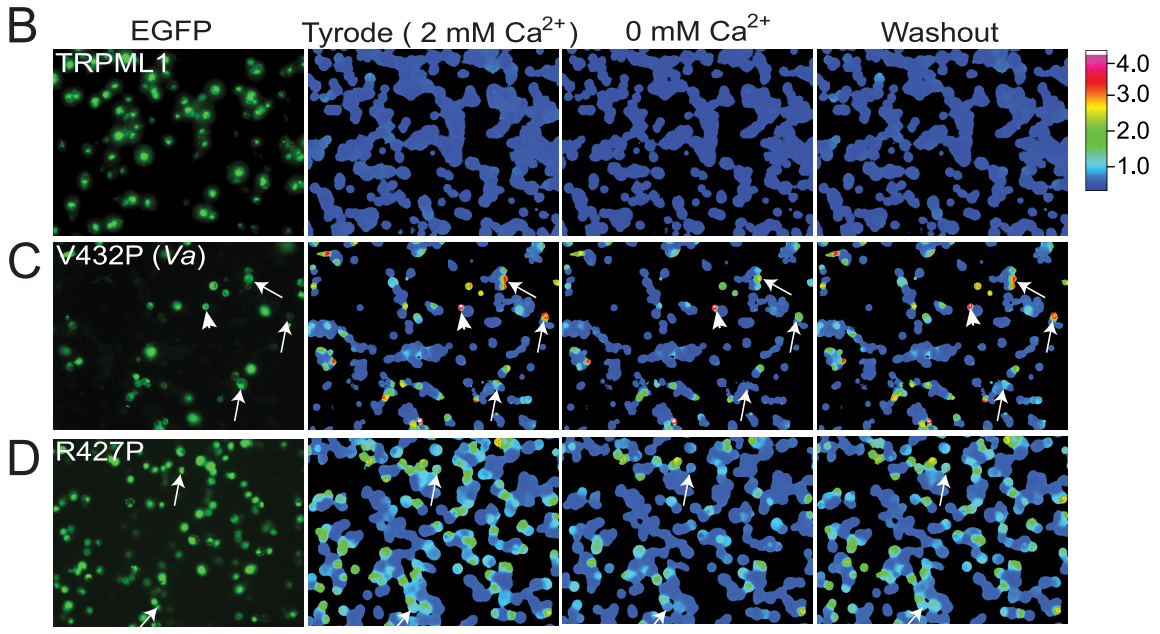
B
EGFP
Tyrode (2 mM Ca2+)
0 mM Ca2+
Washout
TRPML1
4.0
3.0
2.0
1.0
C
V432P (Va)
D
R427P

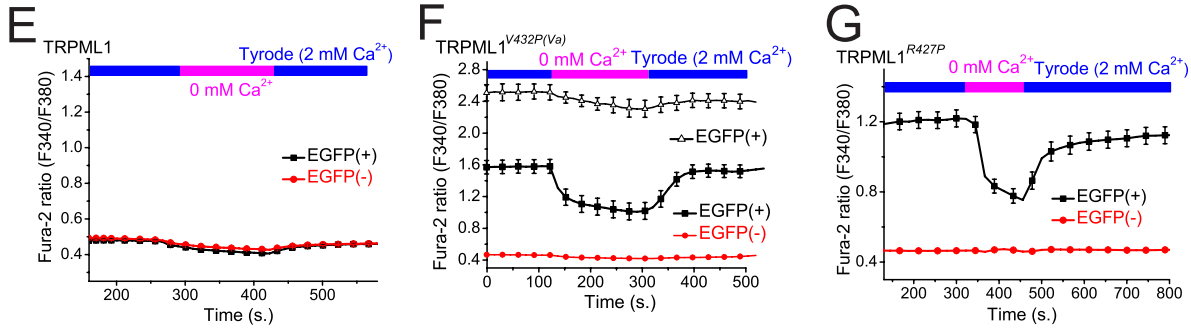
E
TRPML1
Tyrode (2 mM Ca2+)
0 mM Ca2+
EGFP(+)
EGFP(-)
Fura-2 ratio (F340/F380)
Time (s.)
F
TRPML1V432P(Va)
0 mM Ca2+ Tyrode (2 mM Ca2+)
G
TRPML1R427P
0 mM Ca2+Tyrode (2 mM Ca2+)

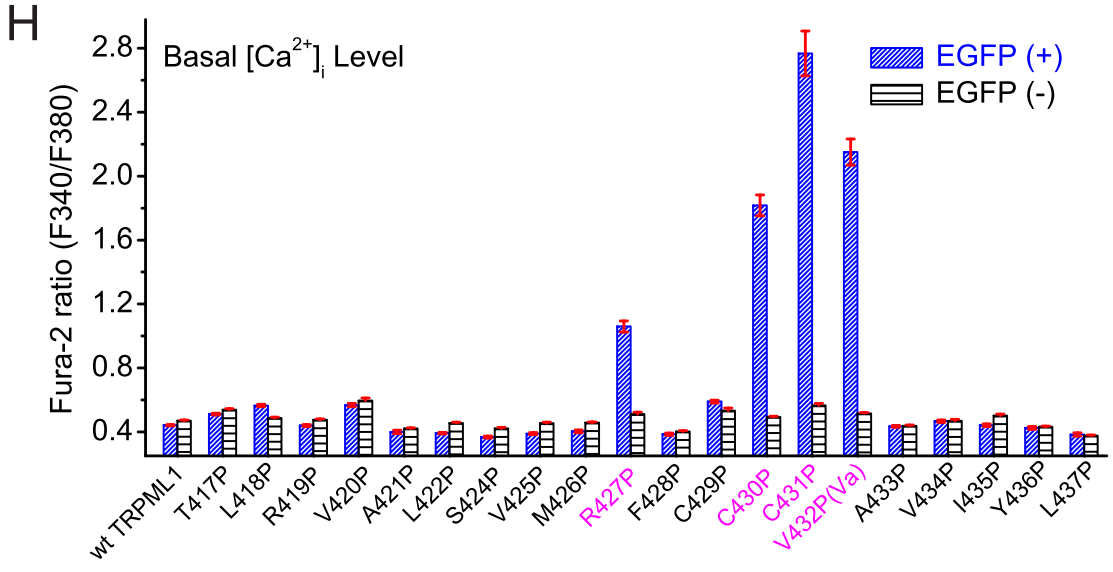
H
Basal [Ca2+]i Level
EGFP (+)
EGFP (-)
Fura-2 ratio (F340/F380)
wt TRPML1
T417P
L418P
R419P
V420P
A421P
L422P
S424P
V425P
M426P
R427P
F428P
C429P
C430P
C431P
V432P(Va)
A433P
V434P
I435P
Y436P
L437P

enlarged LELs (27). Lysosome lumenal-side-out recordings were performed on isolated enlarged LELs, obtained by pressing a patch pipette against a cell and then quickly pulling away from the cell to slice the cell membrane. The enlarged LEL was released into the dish and identified by monitoring the TRPML1-EGFP, TRPML1-mCherry, or Lamp-1 EGFP fluorescence.

Ca^{2+} Imaging—HEK293T cells were loaded with 5 μM Fura-2 AM (Molecular Probes) in culture medium at 37 °C for 60 min. Cells were washed in Tyrode solution for 10–30 min, and the fluorescence intensities at 340 nm (F340) and 380 nm (F380) were recorded on an EasyRatioPro system (Photon Technology International, Birmingham, NJ). Fura-2 ratios (F_{340}/F_{380}) were used to determine $[Ca^{2+}]_i$. The EGFP-positive cells were identified by monitoring fluorescence intensity at 470 nm (F_{470}).

Mn^{2+} Quenching Imaging—HEK293T cells were loaded with 5 μM Fura-2 AM in culture medium at 37 °C for 60 min. The cells were washed in Tyrode solution for 10–30 min, and the fluorescence intensity at 360 nm (F_{360}) was recorded on an EasyRatioPro system. The EGFP-positive cells were identified by monitoring the fluorescence intensity at 470 nm (F_{470}). Mn^{2+} (1 or 10 mM) was added to the low pH Tyrode solution. Images were analyzed using ERP software.

Data Analysis—Data are presented as the mean ± S.E. Statistical comparisons were made using analysis of variance. A p value of <0.05 was considered statistically significant.

RESULTS

To identify additional *Va*-like mutations in TRPML1 that lead to PM expression and measurable whole cell currents, we constructed 20 Pro substitutions near the *Va* locus in the S4–S5 linker and the bottom half of TM5 (Fig. 1*A*). This region was previously implicated in the channel gating of various 6TM channels, including TRP channels (25, 39). Proline-substituted TRPML1 channels were then transiently expressed in HEK-293T cell lines. To monitor expression, TRPML1 was fused to enhanced green fluorescent protein (EGFP) at its N terminus (18, 27). Cells transfected with TRPML1^{Va} or TRPML3^{Va} exhibit elevated intracellular Ca^{2+} levels, *i.e.* Ca^{2+} overload (16, 18). Therefore, our initial screening of Pro substitutions was conducted using Fura-2-based Ca^{2+} imaging. The expressions of TRPML1 and the Pro mutations were confirmed by measuring EGFP fluorescence (F_{470}, Fig. 1*B*).

The basal intracellular Ca^{2+} ($[Ca^{2+}]_i$) levels of wt TRPML1-transfected HEK293T cells were similar to those of non-transfected cells (Fig. 1, *B* and *E*). Thus, consistent with previous localization studies (3, 4, 27), wt TRPML1 was not localized and/or functional at the PM. In contrast, elevated $[Ca^{2+}]_i$ levels were seen in most TRPML1^{Va}-transfected cells (Fig. 1, *C* and *F*) in the standard extracellular Tyrode solution (2 mM Ca^{2+}). Removal of Ca^{2+} from the bath (0 mM Ca^{2+}) rapidly decreased the Fura-2 ratios in most TRPML1^{Va}-transfected cells. However, in a subpopulation of TRPML1^{Va}-transfected cells with high basal $[Ca^{2+}]_i$ levels (fura-2 ratio $>$ 2), Ca^{2+} removal only slightly decreased the Fura-2 ratios (Fig. 1*F*). These cells might have entered an irreversible apoptotic program that was triggered by Ca^{2+} overload (16, 18, 19). Nevertheless, even with TRPML1^{Va}-transfected cells with low basal $[Ca^{2+}]_i$ levels (Fura-2 ratio $<$ 2), Fura-2 ratios never dropped to non-transfected cell levels upon Ca^{2+} removal. These results suggest that TRPML1^{Va} might also have increased basal $[Ca^{2+}]_i$ levels by mobilizing intracellular Ca^{2+} stores. High basal $[Ca^{2+}]_i$ levels were also seen in two other TRPML1 Pro substitutions, TRPML1^{C430P} and TRPML1^{C431P} (Fig. 1*H*). Intermediate $[Ca^{2+}]_i$ levels were observed in another proline substitution, TRPML1^{R427P} (Fig. 1, *D* and *G*). In contrast, no significant alterations in the basal $[Ca^{2+}]_i$ levels were observed in other Pro substitutions (Fig. 1*H*). Thus, the *Va* locus and its vicinity at the cytosolic side may be the only areas susceptible to Pro substitutions. Together, these results indicate that TRPML1^{R427P}, TRPML1^{C430P}, and TRPML1^{C431P} were also TRPML1^{Va}-like GOF mutations.

Next, we investigated whether these channels with proline substitutions were also permeable to heavy metal ions, as is the case for TRPML1^{Va} (27). Because heavy metals such as Mn^{2+} and Fe^{2+} can bind to Ca^{2+}-sensitive Fura-2 dyes with higher affinity, resulting in a strong decrease of the fluorescence via quenching (27, 40), we adopted a fluorescence-based Mn^{2+} quenching assay using Fura-2 (F_{360}). Although no significant quenching was seen in TRPML1-expressing cells (Fig. 2, *A* and *D*), substantial quenching was seen in TRPML1$^{V432P(Va)}$-expressing cells with addition of 1 mM Mn^{2+} (pH 4.6) into a low pH (pH 4.6) external bath solution (Fig. 2, *B* and *E*). The low pH situation was designed to mimic the acidic environment of LEL (27). Increased quenching was observed with the addition of higher concentrations of Mn^{2+} (10 mM, pH 4.6). In contrast, no significant quenching was detected in neighboring EGFP-negative cells (Fig. 2*B*) or mock transfected cells (data not shown). Similarly, fast and substantial quenching was also seen in TRPML1^{C430P}- or

FIGURE 1. **Elevated intracellular Ca^{2+} in HEK293T cells expressing several Pro substitutions of TRPML1 channels.** *A*, alignment of TRPML (TRPML1, TRPML2, and TRPML3) protein sequences in the S4–S5 linker and the bottom half of the TM5. *Stars* (*red*) indicate the locations of the amino acids that, when mutated into Pro, resulted in GOF channel activity. *TM5 (S5)*, putative transmembrane domain 5. *B–D*, elevated intracellular $[Ca^{2+}]$ ($[Ca^{2+}]_i$) in two Pro substitutions of TRPML1. The effect of extracellular Ca^{2+} ($[Ca^{2+}]_o$, 2 mM) on $[Ca^{2+}]_i$ was investigated in HEK293T cells transfected with EGFP-tagged wt TRPML1 and two Pro substitutions (V432P, TRPML1^{V432P}; R427P, TRPML1^{R427P}). TRPML1 protein expression was monitored by the presence of an EGFP signal measured at an excitation of 470 nm (F_{470}). $[Ca^{2+}]_i$ was monitored with Fura2 ratios (F_{340}/F_{380}). Basal $[Ca^{2+}]_i$ in wt TRPML1-transfected cells was similar to non-transfected cells (*B*). In contrast, $[Ca^{2+}]_i$ was significantly elevated in TRPML1^{V432P} (*C*)- and TRPML1^{R427P} (*D*)-transfected cells in the presence of 2 mM extracellular Ca^{2+}. Results are representative of several ($n = 4–8$) independent experiments. *Arrows* indicate the representative cells. *E–G*, in TRPML1^{V432P}- and TRPML1^{R427P}-transfected cells (*F* and *G*), the Fura-2 ratios dropped significantly when $[Ca^{2+}]_o$ was reduced from 2 mM (Tyrode) to 0 mM (nominal Ca^{2+} plus 1 mM EGTA), and gradually recovered with addition of 2 mM Ca^{2+} (Tyrode; washout). The Fura-2 ratios for wt TRPML1 (*E*) did not change significantly after extracellular Ca^{2+} was removed. Note that for TRPML1^{V432P}, cells with Fura-2 ratios $>$2 (in the *empty triangle*) and $<$2 (in the *solid square*) were plotted separately. *H*, average basal $[Ca^{2+}]_i$ in cells transfected with TRPML1 and 20 Pro substitutions in the S4–S5 linker and the bottom half of TM5. Data represent the averaged responses of a total of 40–120 cells from 3–5 independent experiments.

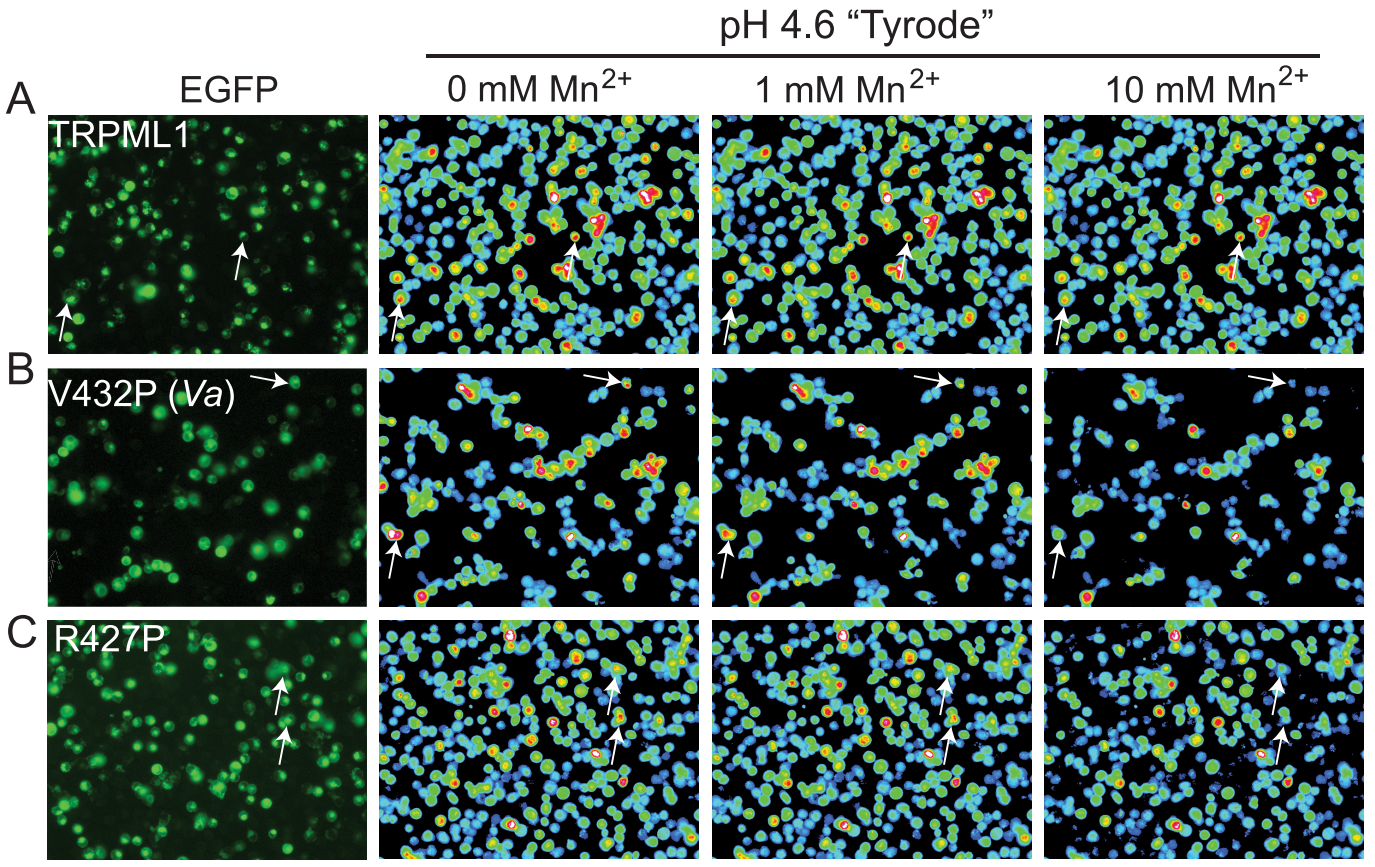
pH 4.6 "Tyrode"
A
EGFP
0 mM Mn2+
1 mM Mn2+
10 mM Mn2+
TRPML1
B
V432P (Va)
C
R427P

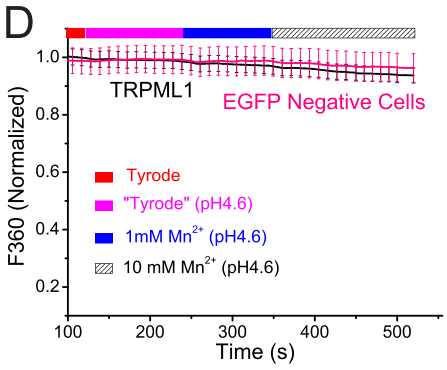
D
TRPML1
EGFP Negative Cells
Tyrode
"Tyrode" (pH4.6)
1mM Mn2+ (pH4.6)
10 mM Mn2+ (pH4.6)
F360 (Normalized)
Time (s)

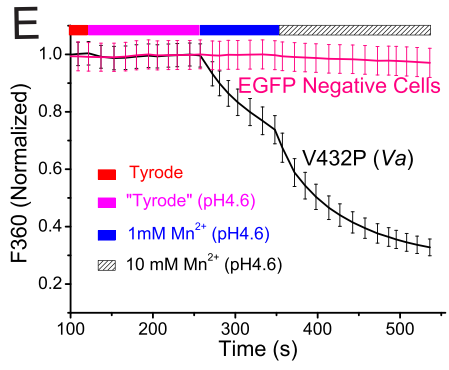
E
EGFP Negative Cells
V432P (Va)
Tyrode
"Tyrode" (pH4.6)
1mM Mn2+ (pH4.6)
10 mM Mn2+ (pH4.6)
F360 (Normalized)
Time (s)

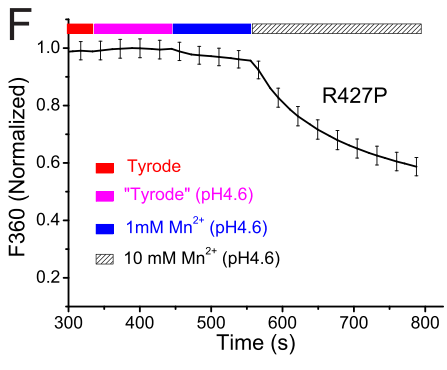
F
R427P
Tyrode
"Tyrode" (pH4.6)
1mM Mn2+ (pH4.6)
10 mM Mn2+ (pH4.6)
F360 (Normalized)
Time (s)

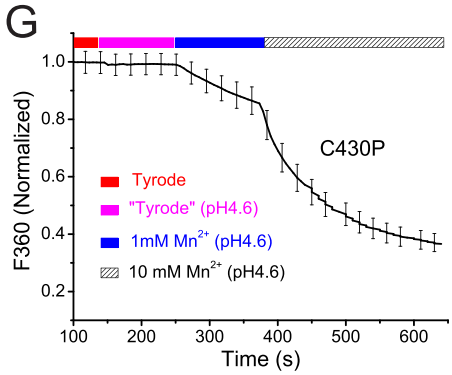
G
C430P
Tyrode
"Tyrode" (pH4.6)
1mM Mn2+ (pH4.6)
10 mM Mn2+ (pH4.6)
F360 (Normalized)
Time (s)

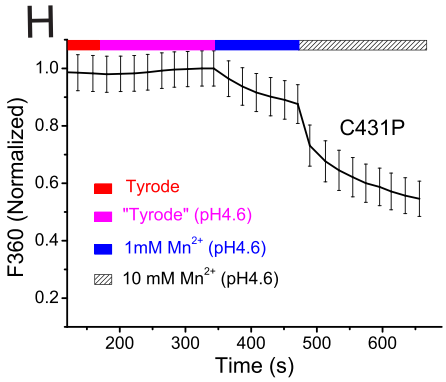
H
C431P
Tyrode
"Tyrode" (pH4.6)
1mM Mn2+ (pH4.6)
10 mM Mn2+ (pH4.6)
F360 (Normalized)
Time (s)

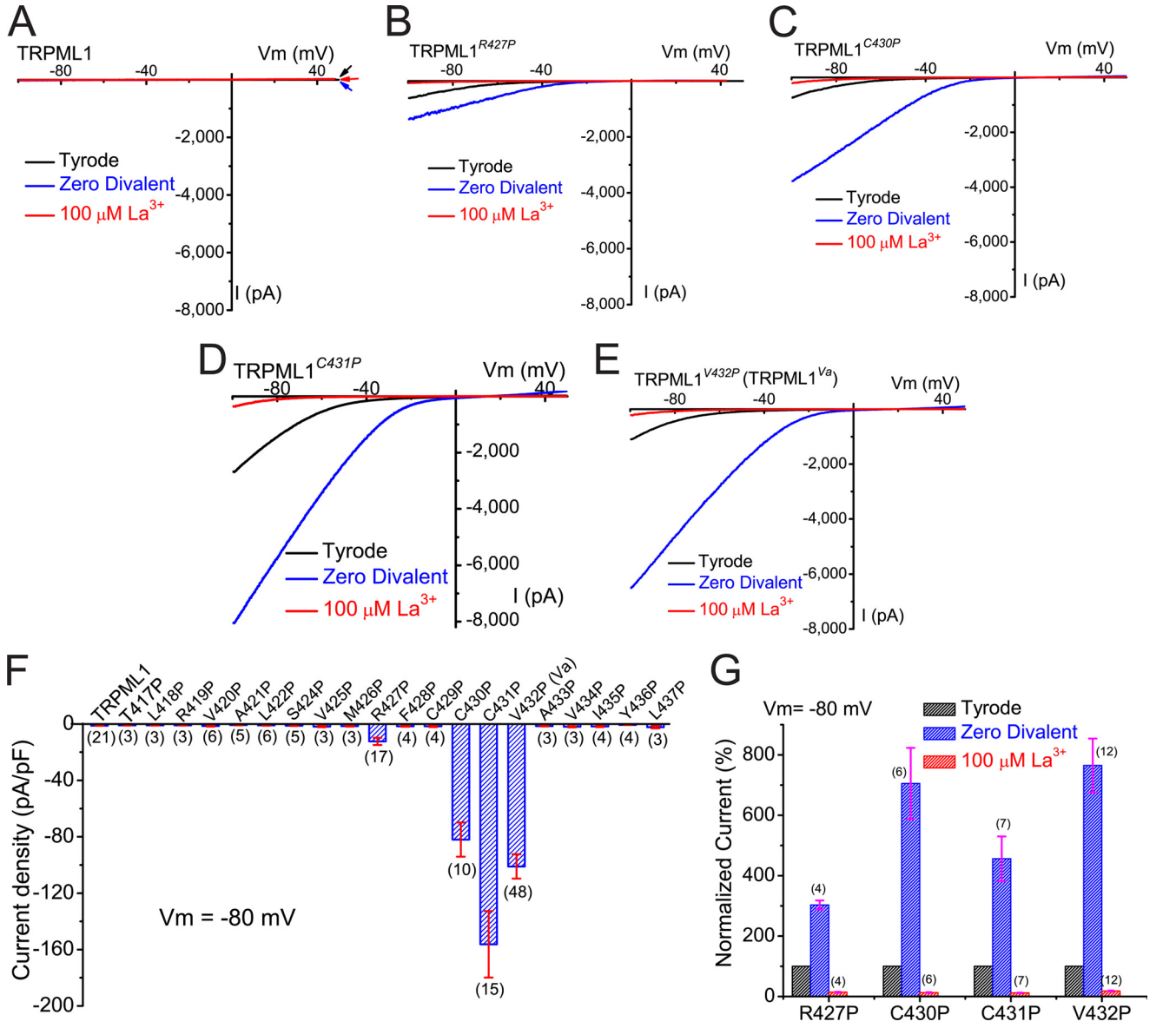

FIGURE 3. **GOF Pro substitutions of TRPML1 channels generated inwardly rectifying whole cell currents.** *A*, no significant whole cell current was seen in a TRPML1-expressing HEK293T cells. Large inwardly rectifying currents were seen in HEK293T cells expressing TRPML1^{R427P} (*B*), TRPML1^{C430P} (*C*), TRPML1^{C431P} (*D*), or TRPML1^{V432P} (*E*). Whole cell currents were elicited by repeated voltage ramps (−100 to +100 mV; 400 ms) with a 4-s interval between ramps. Only a portion of the voltage protocol is shown. Holding potential = 0 mV. *B*, inwardly rectifying whole cell currents were recorded in a TRPML1^{R427P}-expressing cell. The TRPML1^{R427P}-mediated whole cell current ($I_{TRPML1\text{-}R427P}$) was significantly inhibited (>90%) by 100 μM La^{3+}. However, $I_{TRPML1\text{-}R427P}$ was potentiated severalfold when the bath solution was switched from the standard extracellular Tyrode solution to a divalent nominal free (*Zero Divalent*; 0 mM Ca^{2+}/0 mM Mg^{2+}) solution. Currents in the Zero Divalent condition still exhibited strong inward rectification. *C–E*, $I_{TRPML1\text{-}C430P}$, $I_{TRPML1\text{-}C431P}$, and $I_{TRPML1\text{-}V432P}$ were all strongly inhibited by 100 μM La^{3+}, but dramatically potentiated by divalent removal. *F*, average current densities (pA/pF) of 20 Pro substitutions of TRPML1 channels. Only 4 ($I_{TRPML1\text{-}R427P}$, $I_{TRPML1\text{-}C430P}$, $I_{TRPML1\text{-}C431P}$, and $I_{TRPML1\text{-}V432P}$) were significantly larger than I_{TRPML1}, which was not significantly different from the non-transfected cell currents. Currents were measured at −80 mV in the standard extracellular (Tyrode) bath solution and normalized to the size of the cells (capacitance; pF). The number of cells for each Pro substitution is shown in *parenthesis*. *G*, average -fold potentiation by divalent removal (*Zero Divalent*) and La^{3+} inhibition.

TRPML1^{C431P}-expressing cells with addition of 1 mM or 10 mM Mn^{2+} (Figs. 1*H* and 2*G*). These results indicate that, like TRPML1^{Va}, TRPML1^{C430P} and TRPML1^{C431P} could conduct Mn^{2+} in the presence of physiological concentrations of Ca^{2+} (2 mM) and Mg^{2+} (1 mM). A slow but significant Mn^{2+}-induced quenching of Fura-2 fluorescence was seen in

FIGURE 2. **Gain-of-function Pro substitutions of TRPML1 channels cause Mn^{2+} influx in HEK293T cells.** Mn^{2+} entry was assayed with $[Mn^{2+}]_o$-dependent quenching of Fura2 fluorescence at excitation wavelength 360 nm (F_{360}), at which the Fura2 fluorescence intensity is highest. Baseline levels of Fura2 fluorescence reached steady-state in a low pH solution (pH 4.6, low pH Tyrode solution) before adding 1 or 10 mM Mn^{2+}. *A–C*, when 1 or 10 mM Mn^{2+} was added to the bath, significant quenching was seen in cells transfected with TRPML1^{V432P} (*B*, see *arrows* for examples), but not in non-transfected control or wt TRPML1-transfected cells (*A*). For TRPML1^{R427P} (*C*), only small and slow Mn^{2+} quenching was observed with 1 mM Mn^{2+}. However, with 10 mM Mn^{2+}, large quenching was also seen. *D–H*, average responses of EGFP-positive wt and Pro-substituted TRPML1-transfected cells (typically n = 20–40 cells) to 1 or 10 mM Mn^{2+} (pH 4.6). The F_{360} values of the individual cells were averaged and normalized to the baseline value prior to Mn^{2+} addition. One representative response of multiple repeated experiments (n = 3–6) is shown.

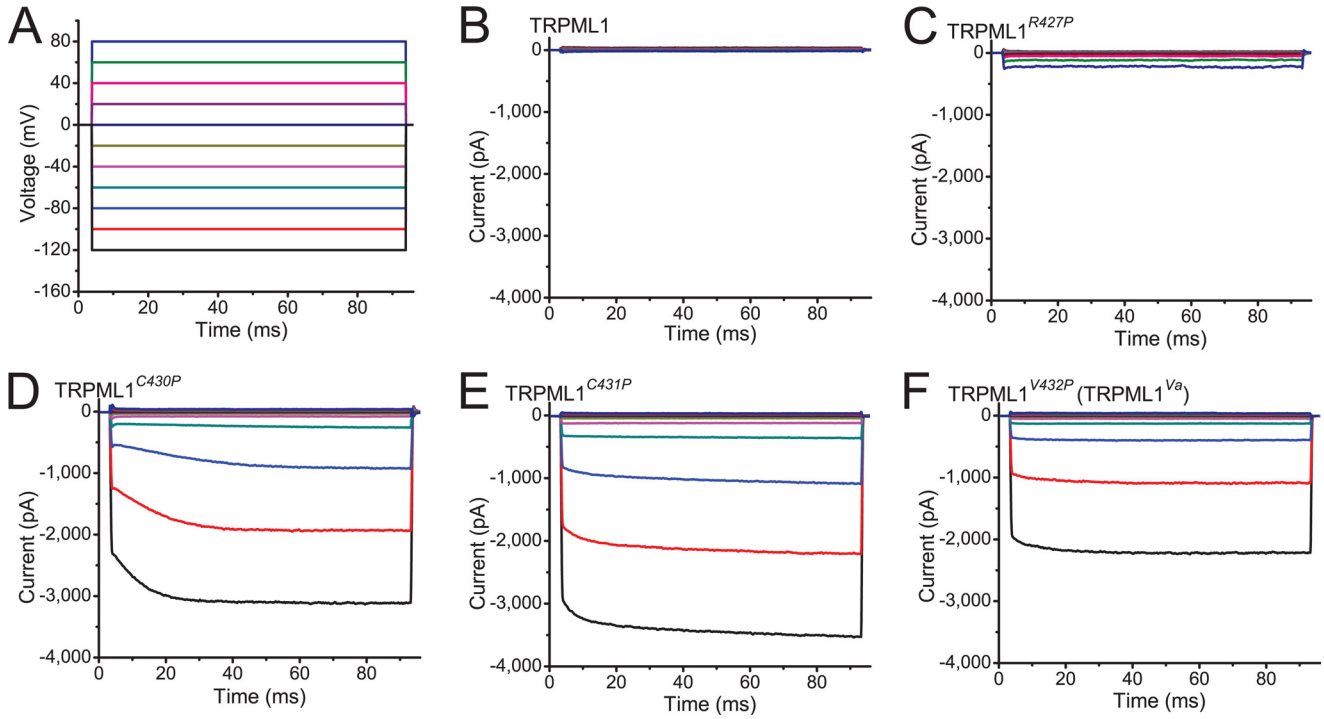

FIGURE 4. **Whole cell current kinetics of TRPML1 Pro substitutions.** *A*, whole cell currents were elicited by voltage steps from −140 mV to +80 mV in increments of 20 mV in the standard extracellular (Tyrode) bath solution. Step duration = 90 ms; holding potential = 0 mV. *B*, no significant step current was seen for I_{TRPML1}. *C*, relatively small inwardly rectifying $I_{TRPML1\text{-}R427P}$. At negative potentials, $I_{TRPML1\text{-}R427P}$ was instantaneously activated and slowly inactivated. *D–F*, large strong inwardly rectifying $I_{TRPML1\text{-}C430P}$ (*D*), $I_{TRPML1\text{-}C431P}$ (*E*), and $I_{TRPML1\text{-}V432P}$ (*F*) were instantaneously activated. No obvious inactivation was seen at any voltage.

TRPML1^{R427P}-expressing cells (Fig. 2, *C* and *F*), suggesting that TRPML1^{R427P} was a partially active Mn^{2+}-permeable channel.

To investigate the detailed mechanisms of Pro-induced GOF TRPML1 channel functions and to compare the biophysical properties of these channels with TRPML1^{Va}, we performed whole cell patch clamp experiments on HEK293T cells expressing these proline substitutions. In response to a voltage ramp protocol, no significant current was detected in TRPML1-expressing cells (Fig. 3*A*). The average TRPML1-mediated current (I_{TRPML1}) at −80 mV was only 1.2 ± 0.2 pA/picofarad (pF) (mean ± S.E., n = 21), which was not significantly different from that of non-transfected cells (data not shown). However, all the GOF Pro mutations displayed strong inwardly rectifying ramp currents (Fig. 3, *B–E*) in a standard, modified Tyrode extracellular bath solution. The average TRPML1^{V432P} (TRPML1^{Va})-mediated current ($I_{TRPML1\text{-}V432P}$) was −99.7 ± 7.3 pA/pF at −80 mV (mean ± S.E., n = 40; Fig. 3*F*). $I_{TRPML1\text{-}C430P}$ and $I_{TRPML1\text{-}C431P}$ were 82.0 ± 12.1 pA/pF (n = 10) and −156.2 ± 23.6 pA/pF (n = 15), respectively. A much smaller current was seen in TRPML1^{R427P}-expressing cells; $I_{TRPML1\text{-}R427P}$ was only 12.3 ± 2.6 pA/pF (n = 17), ~8-fold smaller than $I_{TRPML1\text{-}V432P}$.

A hallmark feature of $I_{TRPML1\text{-}Va}$ is its dramatic potentiation upon removal of divalent cations from the bath solution (18). We therefore studied the effects of divalent removal on GOF proline substitutions. All the GOF currents ($I_{TRPML1\text{-}C430P}$, $I_{TRPML1\text{-}C431P}$, $I_{TRPML1\text{-}V432P}$, and $I_{TRPML1\text{-}R427P}$) were significantly potentiated by divalent removal. However, the degree of potentiation differed considerably for individual GOF mutations. At −80 mV, $I_{TRPML1\text{-}V432P}$ and $I_{TRPML1\text{-}C430P}$ were both potentiated ~ 8-fold while $I_{TRPML1\text{-}C431P}$ and $I_{TRPML1\text{-}R427P}$ were only potentiated ~3- and ~4-fold, respectively. These results suggest that GOF proline substitutions introduce different gating effects on the TRPML1 channels. In contrast, all currents ($I_{TRPML1\text{-}C430P}$, $I_{TRPML1\text{-}C431P}$, $I_{TRPML1\text{-}V432P}$, and $I_{TRPML1\text{-}R427P}$) showed similar sensitivity to the trivalent blockers La^{3+} (Fig. 3, *B–E*) and Gd^{3+} (data not shown). La^{3+} (100 μM) inhibited >80% of $I_{TRPML1\text{-}C430P}$, $I_{TRPML1\text{-}C431P}$, $I_{TRPML1\text{-}V432P}$, and $I_{TRPML1\text{-}R427P}$ (Fig. 3*G*).

We also examined the kinetics and voltage dependence of $I_{TRPML1\text{-}C430P}$, $I_{TRPML1\text{-}C431P}$, $I_{TRPML1\text{-}V432P}$, and $I_{TRPML1\text{-}R427P}$. In response to a voltage step protocol (Fig. 4*A*; from −120 mV to +80 mV with a 20-mV increment), strong inwardly rectifying step currents (Fig. 4, *C–F*) were seen in HEK293T cells expressing GOF proline mutants. Similar to $I_{TRPML1\text{-}V432P}$, $I_{TRPML1\text{-}C430P}$, and $I_{TRPML1\text{-}C431P}$ did not exhibit any significant inactivation over time or in response to voltage changes (Fig. 4, *C–E*). $I_{TRPML1\text{-}R427P}$ behaved differently by exhibiting a certain degree of inactivation at negative potentials (Fig. 4*C*), kinetics that are similar to TRPML3-mediated currents (18). These results suggest that Pro substitutions affect the pore/gating properties of the TRPML1 channel.

Because wt TRPML1 localizes to the acidic LEL of cells, the proton dependence of TRPML1 is likely to be of physiological importance (22). TRPML1 has been reported to be a proton channel (32, 33) or a cation channel that is inhibited by low pH (28, 30). However, we recently showed that TRPML1^{Va} is impermeable to protons but up-modulated by low pH (18, 27).

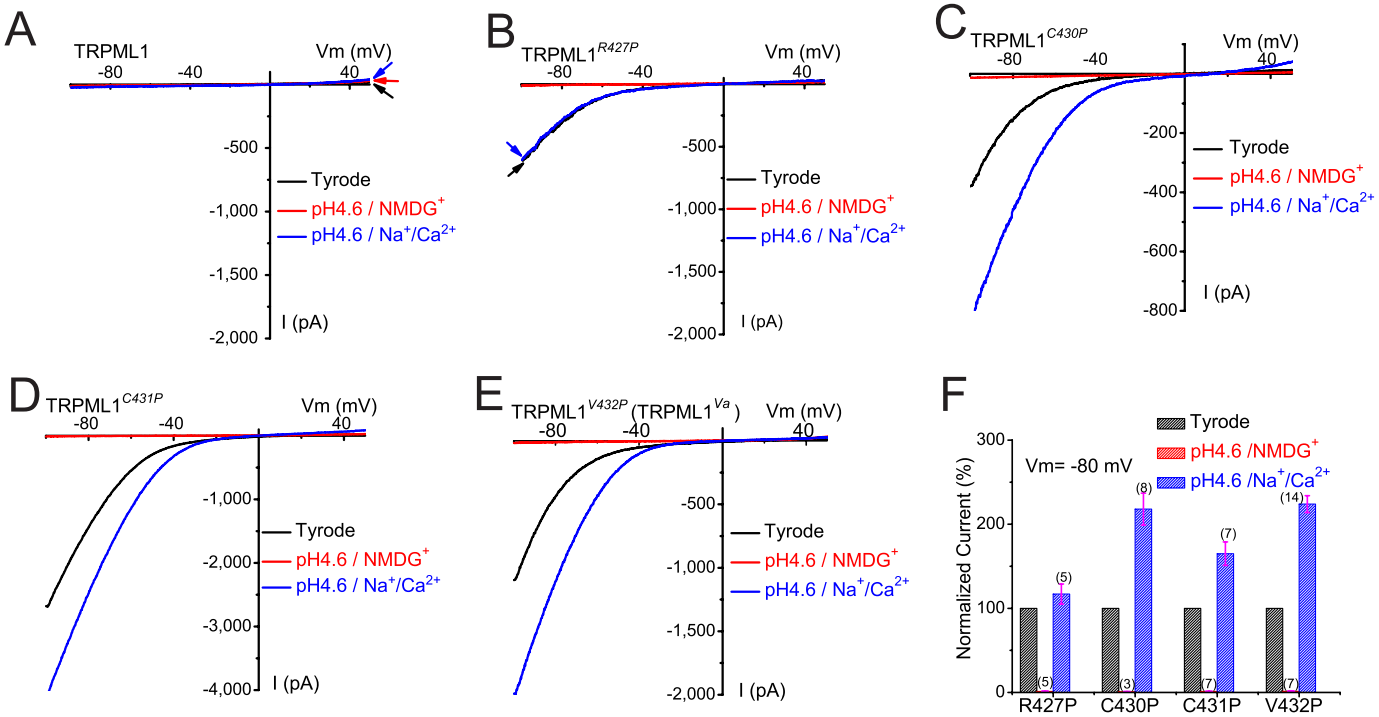

FIGURE 5. **GOF Pro substitutions of TRPML1 channels are proton-impermeable but modulated by protons.** *A*, no significant current was detected in TRPML1-expressing cells in Tyrode, low pH Tyrode (pH 4.6), or low pH NMDG (Na^+-free, Ca^{2+}-free, pH 4.6) solutions. *B*, no significant inward current was detected in $TRPML1^{R427P}$-expressing cells in a low pH NMDG solution. $I_{TRPML1\text{-}R427P}$ was relatively insensitive to low pH. *C–E*, although $I_{TRPML1\text{-}C430P}$, $I_{TRPML1\text{-}C431P}$, and $I_{TRPML1\text{-}V432P}$ were enhanced at low pH (pH 4.6), in a low pH NMDG solution no significant current was detected in HEK293T cells expressing $TRPML1^{C430P}$, $TRPML1^{C431P}$, or $TRPML1^{V432P}$. *F*, normalized current amplitude of $I_{TRPML1\text{-}R427P}$, $I_{TRPML1\text{-}C430P}$, $I_{TRPML1\text{-}C431P}$, and $I_{TRPML1\text{-}V432P}$ in the low pH solutions (low pH Tyrode and low pH $NMDG^+$ solutions).

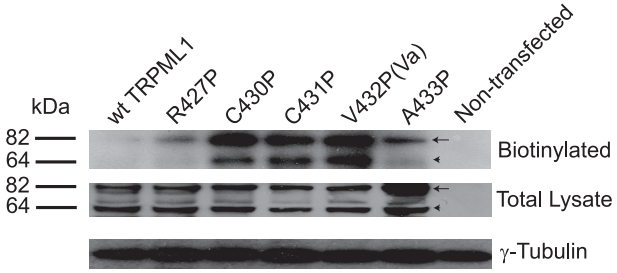

FIGURE 6. **GOF Pro substitutions of TRPML1 exhibit high plasma membrane expression.** Cell lysates were prepared from HEK293T cells transfected with EGFP-TRPML1, EGFP-$TRPML1^{R427P}$, $TRPML1^{C430P}$, $TRPML1^{C431P}$, $TRPML1^{V432P}$, or $TRPML1^{A433P}$. Cell surface membrane proteins were prelabeled with biotin. The Western blot was probed with an anti-EGFP antibody. Both biotinylated and total TRPML1 are shown. *Arrows* indicate the ~80-kDa band of EGFP-TRPML1 or other EGFP-TRPML1-derived mutant proteins. *Arrowheads* indicate a band of ~60 kDa, probably resulting from a cleavage product of EGFP-TRPML1 or its mutants. *Bottom panels* show the loading controls probed by anti-γ-tubulin.

It is possible, although unlikely, that the V432P (*Va*) mutation somehow masks the proton-permeation pathway and alters the pH regulation. We did not observe the wt TRPML1 current in standard whole cell recordings, but did detect the current in the whole-lysosome configuration (27). Unfortunately, the latter is a very difficult configuration for studying proton regulation and permeation. Having obtained additional GOF mutations, we next tested the proton-dependent properties of these channels.

To mimic the acidic environments of the endosomes and lysosomes that the extracellular side (analogous to the intralysosomal luminal side) of the wt TRPML1 protein is exposed to, extracellular solutions were adjusted to pH 4.6 (the approximate lysosomal luminal pH). Background pH-activated Cl^- conductance was reduced by using $gluconate^-$ or MES^- to replace most of the Cl^- (remaining $[Cl^-]_o = 5–10$ mM) in all low pH bath solutions (18, 27, 41). Consistent with our previous report (18), $I_{TRPML1\text{-}V432P}$ was potentiated by ~2.4-fold by low pH (Fig. 5*E*). Similarly, proton-induced potentiation was also seen for two other GOF channels, $I_{TRPML1\text{-}C430P}$ and $I_{TRPML1\text{-}C431P}$ (Fig. 5, *C–F*). In contrast, no evident proton potentiation was seen for $I_{TRPML1\text{-}R427P}$ (Fig. 5*B*).

No significant inward current was detected in any of the GOF TRPML1 channels when $NMDG^+$ was the only major cation in the bath (pH 4.6, Fig. 5, *B–F*). At −80 mV, the current amplitude in the low pH NMDG solution was usually <30 pA, much smaller than the current in the low pH Tyrode solution (usually >1000 pA), but comparable to the current under the same conditions in non-transfected cells. These results indicate that GOF TRPML1 channels do not exhibit any significant proton permeability and are thus proton-impermeable.

Western blot analyses on HEK293T cells expressing wt or mutant TRPML1 indicated that the TRPML1 Pro substitutions did not dramatically change protein expression, because the total expression level of each GOP mutation protein was comparable to that of wt TRPML1 (Fig. 6). Two other potential explanations for why whole cell currents were recorded in the GOF Pro mutant TRPML1-expressing cells, but not in the wt TRPML1-expressing cells are that the GOF mutations may have increased either the channel surface expression (trafficking hypothesis) or the channel activity (gating hypothesis). To distinguish between these possibilities, we investigated the sub-

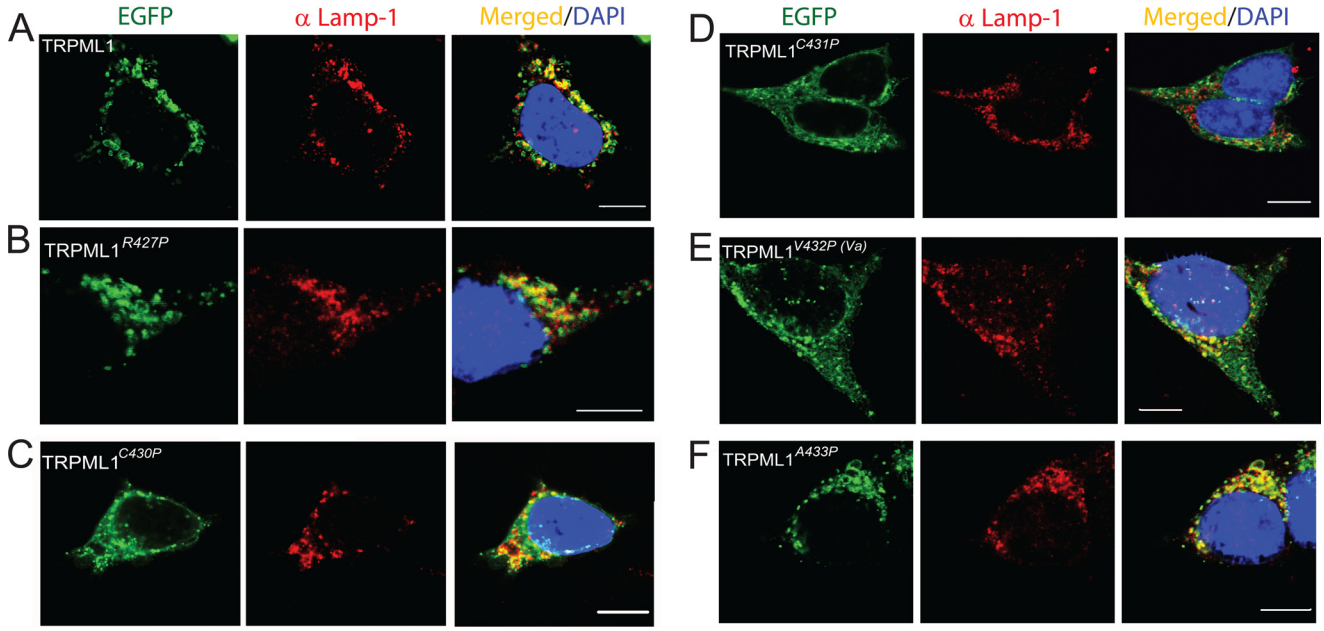

FIGURE 7. **Subcellular localizations of wt and Pro-substituted TRPML1 proteins.** *A–F*, confocal images of fixed HEK293T cells transfected with EGFP-TRPML1, EGFP-TRPML1^{R427P}, EGFP-TRPML1^{C430P}, EGFP-TRPML1^{C431P}, EGFP-TRPML1^{V432P}, or EGFP-TRPML1^{A433P}. Cells were immunostained using a Lamp-1 antibody, a late endosomal and lysosomal marker, and loaded with the nuclear marker 4′,6-diamidino-2-phenylindole. *A*, EGFP-TRPML1 primarily localized in Lamp-1-positive compartments. *B*, EGFP-TRPML1^{R427P}, like EGFP-TRPML1, also primarily localized in Lamp-1-positive compartments. *C*, EGFP-TRPML1^{C430P} localized throughout the cell, including in Lamp-1-positive compartments. *D*, EGFP-TRPML1^{C431P} localized throughout the cell. *E*, EGFP-TRPML1^{V432P} localized throughout the cell, including in Lamp-1-positive compartments. *F*, EGFP-TRPML1^{A433P}, like EGFP-TRPML1, primarily localized in Lamp-1-positive compartments. *Scale bar* = 10 μm.

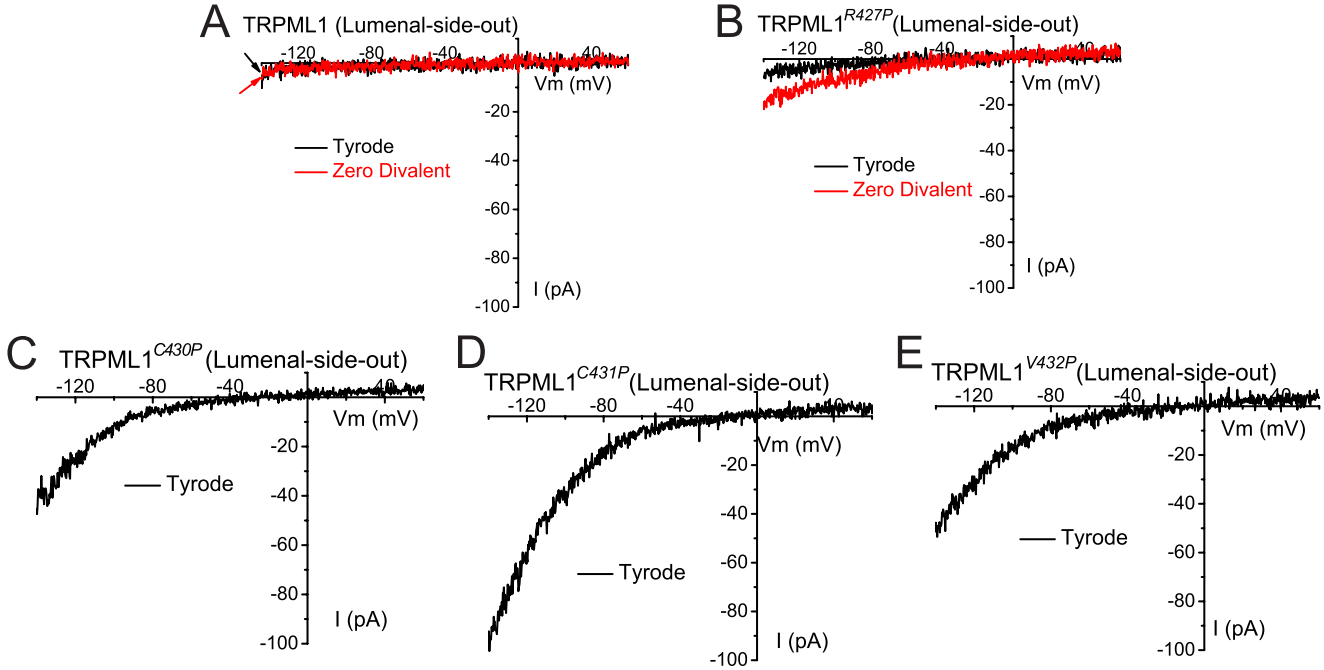

FIGURE 8. **GOF TRPML1 Pro substitutions also display high channel activities in late endosomes and lysosomes.** *A*, lysosomal *I*TRPML1 under (lysosome) lumenal-side-out configuration. The lumenal-side-out patch was exposed to Tyrode solution or a divalent nominal free (Zero Divalent; 0 mM Ca^{2+}/0 mM Mg^{2+}) solution. A Cs^{+}-based solution (147 mM Cs-MES) was used as a pipette solution for both configurations. *B*, lysosomal *I*TRPML1-R427P was detectable in a Zero Divalent solution. *C–E*, lysosomal $I_{TRPML1\text{-}C430P}$ (*C*), $I_{TRPML1\text{-}C431P}$ (*D*), and $I_{TRPML1\text{-}V432P}$ (*E*) were inwardly rectifying.

cellular localization of all GOF mutations, as well as some other neighboring Pro substitutions that failed to produce whole cell currents (non-GOF Pro substitutions (Fig. 7)). Consistent with our previous reports (27), the confocal imaging of EGFP-TRPML1-transfected, fixed HEK293T cells indicated that TRPML1 primarily localized in Lamp-1-positive compartments, *i.e.* the late endosomes and lysosomes (Fig. 7*A*). The Pearson's coefficient of colocalization between Lamp-1 and wt TRPML1 was >0.8 (supplemental Table 1). Similar colocalization was also seen in cells transfected with EGFP-TRPML1^{A433P} (Fig. 7*F*). In contrast, EGFP-TRPML1^{C430P}, EGFP-TRPML1^{C431P}, and EGFP-TRPML1^{V432P} were all localized in compartments throughout the

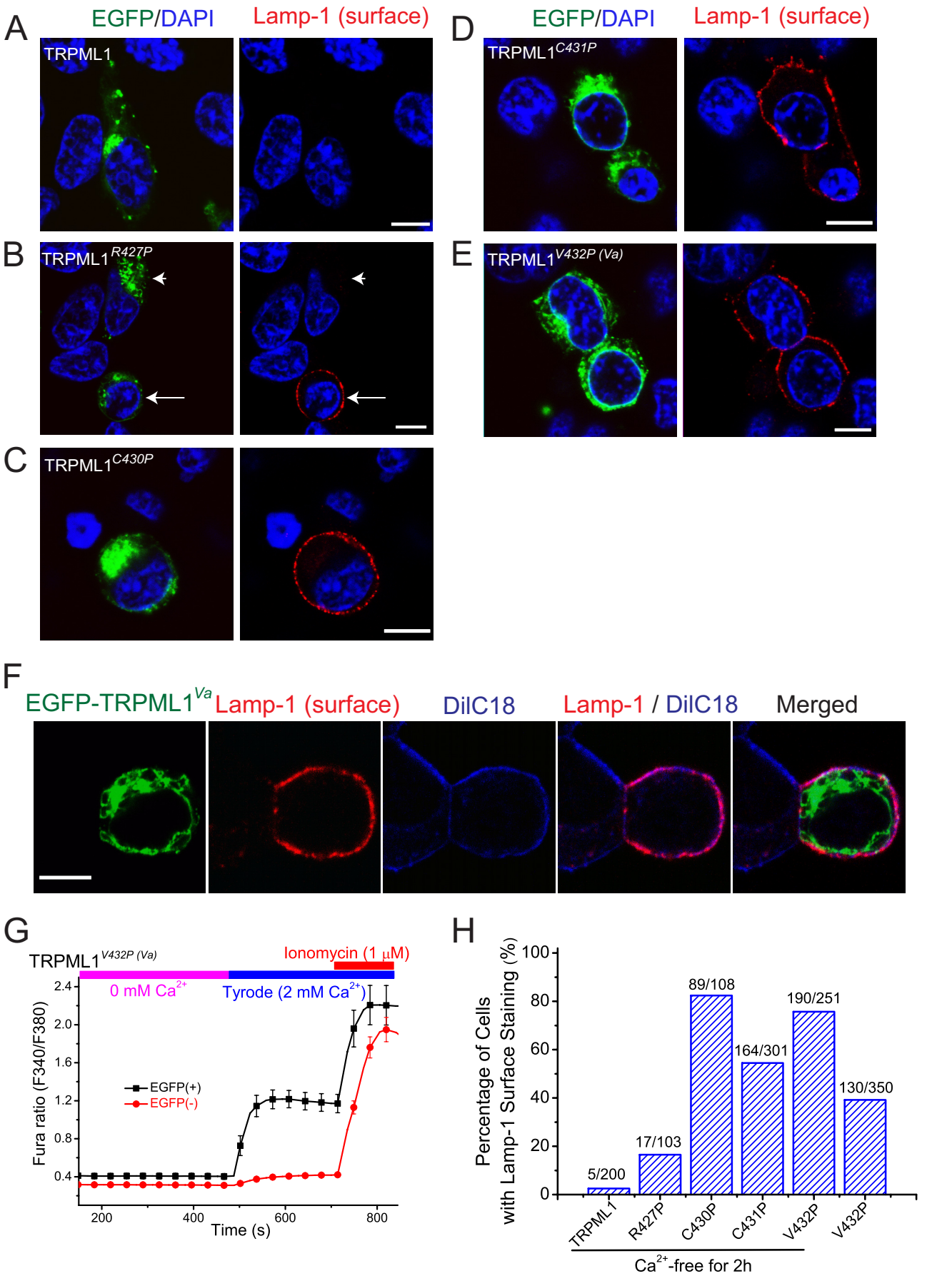
A
EGFP/DAPI
Lamp-1 (surface)
TRPML1
B
TRPML1R427P
C
TRPML1C430P
D
EGFP/DAPI
Lamp-1 (surface)
TRPML1C431P
E
TRPML1V432P (Va)
F
EGFP-TRPML1Va
Lamp-1 (surface)
DilC18
Lamp-1 / DilC18
Merged
G
TRPML1V432P (Va)
Ionomycin (1 μM)
0 mM Ca2+
Tyrode (2 mM Ca2+)
EGFP(+)
EGFP(-)
Fura ratio (F340/F380)
Time (s)
H
Percentage of Cells with Lamp-1 Surface Staining (%)
5/200
17/103
89/108
164/301
190/251
130/350
TRPML1
R427P
C430P
C431P
V432P
V432P
Ca2+-free for 2h

cells, including Lamp-1-positive compartments (Fig. 7, *C–E*). The Pearson's coefficients of colocalization for these GOF Pro substitutions were only ~0.3–0.4 (supplemental Table 1). EGFP-TRPML1^{R427P} exhibited an intermediate level of colocalization. Thus, the GOF channel function and the mislocalization of TRPML1 proteins appeared to be interrelated.

To further investigate the effect of Pro substitutions on channel trafficking, we measured surface expression of TRPML1 channels by the standard biotinylation method (see "Materials and Methods"). Little or no expressed protein was biotinylated for wt TRPML1 or TRPML1^{A433P} (Fig. 6). In contrast, significant amount of protein was biotinylated for all GOF Pro substitutions (TRPML1^{C430P}, TRPML1^{C431P}, and TRPML1^{V432P}). On average, the amount of surface-expressed (biotinylated) TRPML1 proteins was ~10-fold less (11 ± 3%, $n = 3$) than that of TRPML1^{V432P}. An intermediate level of biotinylation was seen for TRPML1^{R427P}. These results suggest that Pro substitutions, either directly or indirectly, increased surface expression of TRPML1 channels.

To explore the primary effect of Pro substitutions on TRPML1, we performed patch clamp recordings directly on native LEL membranes (Fig. 8). In TRPML1^{Va}-expressing enlarged LEL, large inwardly rectifying currents were seen under the lysosome lumenal-side-out configuration. Similar currents were seen in TRPML1^{C430P}- or TRPML1^{C431P}-positive LEL vacuolar membranes (Fig. 8, *C* and *D*). Conversely, no significant current was observed in wt TRPML1 or TRPML1^{R427P}-expressing LEL (Fig. 8, *A* and *B*). A small inwardly rectifying current was detectable for TRPML1^{R427P} after the divalent cations were removed from the bath solution (Zero Divalent (Fig. 8*B*)). All TRPML1 variants (TRPML1, TRPML1^{R427P}, and other GOF TRPML1 channels) appeared to have comparable expression levels in LEL, as reflected in the EGFP fluorescence intensity. These results suggest that one of the primary, if not the sole, effects of the Pro substitutions was on TRPML channel gating.

One possible route by which the GOF mutations could get to the PM is by enhanced fusion of lysosomes with these mutant TRPML1 channels. If this is occurring, then other lysosomal membrane proteins might also be detected in the PM of cells expressing GOF mutants. To probe this possibility, we used Lamp-1 surface staining to monitor the PM trafficking of lysosomal membrane proteins, such as TRPML1 (37). Non-transfected or TRPML1-transfected cells did not exhibit significant Lamp-1 surface staining (Fig. 9*A*), suggesting a low rate of lysosomal exocytosis. However, in cells transfected GOF Pro mutants, evident punctuate Lamp-1 staining was seen in most transfected cells (Fig. 9, *B–E*). TRPML1^{R427P} exhibited an intermediate level of Lamp-1 surface staining (Fig. 9, *B* and *H*). The Lamp-1 staining appeared to be in the cell surface based on its colocalization with a plasma membrane marker DilC$_{18}$ (Fig. 9*F*). Pro substitutions increased both whole cell and whole lysosome currents, resulting in increases of both intralysosomal Ca^{2+} release and Ca^{2+} entry. To separate these two potential distinct effects on lysosomal exocytosis, we performed the experiments under Ca^{2+}-free conditions by removing external Ca^{2+} in the culture medium. Under this condition, the global Ca^{2+} level of TRPML1^{Va}-transfected cells was only slightly above the resting Ca^{2+} level of non-transfected cells (Fig. 9*G*). Interestingly, Lamp-1 surface staining in TRPML1^{V432P}-transfected cells was even enhanced under Ca^{2+}-free conditions (Fig. 9*H*). These results suggest that GOF Pro mutations induce a high level of lysosomal exocytosis via a mechanism that is dependent on lysosomal Ca^{2+} release.

DISCUSSION

In this study, by performing systemic Pro substitution on 20 amino acid residues around the *Va* spot, we obtained several additional GOF *Va*-like mutations that displayed GOF activities at both the PM and endolysosomal membranes. Each Pro-substituted GOF TRPML1 channel displayed inwardly rectifying currents that were carried by Ca^{2+} or Mn^{2+}, but not by protons. Although wild-type TRPML1 and non-GOF Pro substitutions localized exclusively in LEL, the GOF mutations with high constitutive activities exhibited significant surface (PM) expression. Consistent with a role of TRPML1 in Ca^{2+}-dependent lysosomal exocytosis, Lamp-1 surface staining was dramatically increased in cells expressing GOF TRPML1 channels. We conclude that TRPML1 is an inwardly rectifying, proton-impermeable, cation channel that may be gated by unidentified cellular mechanisms through a conformational change in the cytoplasmic face of the TM5.

Although the genetic importance of TRPML proteins is well established (8–10, 13, 14, 21, 25, 43), their normal physiological functions remain unclear. At least three important queries remain to be addressed for these putative intracellular ion channels: what their biophysical and permeation properties are, how they are gated or activated by cellular cues, and how they are trafficked to the LEL and/or PM. In contrast with most other TRP channels, these three aspects of TRPML channels are interrelated. For example, the exocytosis of lysosomal contents is regulated by the release of intralysosomal Ca^{2+} into the cytosol (22, 37). Therefore, cytosolic or lumenal stimulation (gating) of a Ca^{2+}-permeable lysosomal channel ("permeation") would trigger the surface expression (trafficking) of this channel protein. In addition, inwardly rectifying (permeation) but not outwardly rectifying Ca^{2+} channels are more likely to mediate the release of intralysosomal Ca^{2+} from the lumen into the cytosol.

FIGURE 9. **High levels of lysosomal exocytosis in HEK cells expressing GOF Pro substitutions of TRPML1.** *A–E*, TRPML1 and Pro substitutions were transiently transfected in HEK293T cells. To reduce the cellular toxicity of GOF mutations due to Ca^{2+} overload, these experiments were performed 17–20 h after transfection. Before immunostaining analysis, cells were kept in Ca^{2+}-free medium (nominal 0 mM Ca^{2+}, 1 mM EGTA) for 2–6 h. The exocytosis of lysosomal content (lysosomal exocytosis) was monitored by immunostaining of Lamp-1 in non-permeabilized cells using a Lamp-1 antibody whose epitope is located on the lumenal side. *A*, no significant Lamp-1 staining was seen in TRPML1-trasnfected cells. *B*, for TRPML1^{R427P}-trasnfected cells, some exhibited significant Lamp-1 surface staining (see *arrows* for examples), whereas others didn't (see *arrowheads* for examples). Lamp-1 staining in cells transfected with TRPML1^{C430P} (*C*), TRPML1^{C431P} (*D*), and TRPML1^{V432P} (*E*). *F*, Lamp-1 surface staining in TRPML1^{V432P}-transfected cells was colocalized with the plasma membrane marker DilC18. *G*, slightly elevated $[Ca^{2+}]_i$ in TRPML1^{V432P}-transfected cells that were preincubated in Ca^{2+}-free medium for 2–6 h. *H*, percentage of EGFP-positive cells with Lamp-1 surface staining under standard (2 mM external Ca^{2+}) and Ca^{2+}-free conditions.

Properties of TRPML channels may explain some of the controversies in the TRPML field. For example, due to the coupled mechanisms of gating and trafficking, intracellular TRPML channels may also appear in the PM depending on the presence of certain cellular mechanisms that can activate these channels. These activation cues might be generated upon certain stimulations or may be present only in specialized cells. Because the excess overexpression of proteins may dysregulate the cellular pathways, the trafficking and properties of TRPML channels might be affected in an expression system-specific manner. Because the steady-state location of TRPML channels are LEL (4, 16–19, 27), it is likely the primary function of TRPML is endolysosomal. Nevertheless, it remains possible that TRPML channels might also function in the PM in certain cell types under specific cellular stimulations.

Lysosomes containing constitutively active TRPML1 channels may undergo un-regulated exocytosis. Lysosomes can undergo Ca^{2+}-dependent regulated exocytosis in almost all studied cell types (37, 44). Although intralysosomal Ca^{2+} release is the proposed initiative step, the triggering mechanism for lysosomal Ca^{2+} release remains unknown. Lysosomes are heterogeneous, but it was recently shown that TRPML1-positive lysosomes can undergo exocytosis (36). Moreover, TRPML1 itself appears necessary for exocytosis. It is possible that, upon unidentified cellular stimulations, TRPML1 mediates intralysosomal Ca^{2+} release to trigger lysosomal exocytosis. Because GOF TRPML1 Pro substitutions displayed high channel activity in LEL, exocytosis is expected to be high for these lysosomes, which was demonstrated in the current study by using Lamp-1 surface staining. Consistent with this, Pro substitutions with large currents, *i.e.* $TRPML1^{C430P}$, $TRPML1^{C431P}$, and $TRPML1^{V432P}$, all appeared to be localized throughout the cells, including the PM, as shown in the biotinylation experiment and reflected by their large whole cell currents. In contrast, non-GOF ($TRPML1^{A433P}$) and low activity ($TRPML1^{R427P}$) Pro substitutions mainly localized in the LEL. It is worth noting that only a small portion of TRPML1 can be biotinylated. Consistent with this, immunostaining analysis suggests that the amount of Lamp-1 in the PM is only a small portion of the total Lamp-1 levels (data not shown). Therefore, only a small portion of GOF TRPML1 channels may have been inserted into the PM. Yet, large whole cell currents are generated. Because appearance of Lamp-1 surface staining is increased under Ca^{2+}-free conditions, it is most likely that the increase of lysosomal Ca^{2+} release directly results in the enhanced lysosomal exocytosis (37). Lysosomal exocytosis is known to play important roles in several physiological processes, including neurotransmitter release and membrane repair (36, 37, 45). It is conceivable that TRPML1 may be involved in these physiological functions by mediating intralysosomal Ca^{2+} release. Finally, in addition to the PM, lysosomes can also exchange materials with other vesicular compartments such as early and late endosomes (22, 23). Therefore, TRPML1 might also be involved in these cellular processes. The constitutive Ca^{2+} channel activity of GOF Pro substitutions may have altered these intracellular trafficking pathways, contributing to the appearance of GOF Pro mutations in non-lysosomal intracellular compartments. In addition, TRPML channels may also be present in Golgi and endoplasmic reticulum during biosynthetic processes, which could also be Ca^{2+}- dependent.

Pro substitutions in TRPML1 cause two distinct but correlative effects: increased surface expression and GOF channel function. Recordings in LEL indicate that Pro substitutions induce GOF in the channel activity. So this change of channel activity is likely to be the principal or initial effect of Pro substitutions. Both surface expression of TRPML1 (measured with biotinylation) and Lamp-1 surface staining are correlated with the GOF channel activity. Although it is possible, it is very unlikely that all Pro substitutions interfered the biosynthetic processing of TRPML1 proteins concurrently with the change of channel activity. Thus the simplest explanation of these results is that these effects, *i.e.* appearance of TRPML1 and Lamp-1at the plasma membrane, are secondary to the change of channel activity. The helix-breaking effect of Pro introduction may have interfered the conformational changes that normally occurred during channel activation gating. GOF Pro substitutions could have locked the TRPML1 channel in an unregulated and open state. Such mechanisms have been demonstrated in several other 6TM cation channels (16, 25, 46). All GOF Pro substitutions are located in the cytoplasmic face of the TM5. Thus, it is possible that unidentified cellular mechanisms may activate wt TRPML1 via an conformational change in this S4–S5 linker region, which has been previously implicated in the gating of various 6TM cation channels (25, 39). Increased TRPML1 channel activity or activation of TRPML1 may trigger intralysosomal Ca^{2+} release, and subsequently the appearance of TRPML1 and Lamp-1 at the plasma membrane.

The "gating-trafficking coupling theory" offers a potential explanation for the observed differences between TRPML3 and TRPML1. The substantial whole cell TRPML3 current (17, 18) may result from the higher constitutive basal channel activity of TRPML3, especially during overexpression. In contrast, TRPML1 is likely to be more tightly regulated. Therefore, the wt TRPML1 current cannot be reliably detected at the PM of mammalian cells (3, 18). In this regard, it would be misleading to refer to TRPML3 as a PM channel and TRPML1 as an LEL channel. Compared with TRPML3, which is readily trafficked to the PM, TRPML1 has far fewer GOF Pro substitutions in the area of the S4–S5 linker and TM5 (see Fig. 3 of Ref. 16). The exact boundary between the cytosolic S4–S5 linker and TM5 may not be accurately predicted using bioinformatics, especially because LEL membranes are different from PMs (23). However, the GOF Pro substitutions in TRPML1 appeared to be restricted to this boundary. It is plausible that TRPML1 channels are gated by unknown mechanisms via a conformation change close to the boundary.

Although major questions remain regarding the gating and trafficking mechanisms of TRPML channels, the permeation properties TRPML channels are relatively clear. Our results also suggest that some Pro substitutions may affect the channel pore properties. Therefore, caution is necessary when extrapolating the properties of GOF TRPML1 channels to the wt TRPML1 channel in LEL. For example, although very unlikely, wt TRPML1 in LEL may not be a pH-activated channel. However, because all GOF TRPML1 channels are proton-impermeable and Pro substitutions in these sites (Arg-427, Cys-430,

Cys-431, and Val-432) are not likely to disrupt any proton permeation pathway, TRPML1 is unlikely to be a proton channel. Consistent with the I-V of wt TRPML1 in LEL, all the GOF TRPML1 channels are inwardly rectifying. Nevertheless, recent evidence suggests that the permeation might be affected by gating in certain TRP channels (42). As a family of physiologically important channels, TRPML may represent a unique model for studying the relationships between permeation, gating, and trafficking.

Acknowledgments—We are grateful to Rich Hume, John Kuwada, Mohammed Akaaboune, and Cathy Collins for constructive comments. We appreciate the encouragement and helpful comments from other members of the Xu laboratory.

REFERENCES

1. Clapham, D. E. (2003) *Nature* **426,** 517–524
2. Montell, C. (2005) *Sci. STKE 2005,* re3
3. Pryor, P. R., Reimann, F., Gribble, F. M., and Luzio, J. P. (2006) *Traffic* **7,** 1388–1398
4. Venkatachalam, K., Hofmann, T., and Montell, C. (2006) *J. Biol. Chem.* **281,** 17517–17527
5. Vergarajauregui, S., and Puertollano, R. (2006) *Traffic* **7,** 337–353
6. Nilius, B., Owsianik, G., Voets, T., and Peters, J. A. (2007) *Physiol. Rev*. **87,** 165–217
7. Zeevi, D. A., Frumkin, A., and Bach, G. (2007) *Biochim. Biophys. Acta* **1772,** 851–858
8. Bargal, R., Avidan, N., Ben-Asher, E., Olender, Z., Zeigler, M., Frumkin, A., Raas-Rothschild, A., Glusman, G., Lancet, D., and Bach, G. (2000) *Nat. Genet.* **26,** 118–123
9. Bassi, M. T., Manzoni, M., Monti, E., Pizzo, M. T., Ballabio, A., and Borsani, G. (2000) *Am. J. Hum. Genet.* **67,** 1110–1120
10. Sun, M., Goldin, E., Stahl, S., Falardeau, J. L., Kennedy, J. C., Acierno, J. S., Jr., Bove, C., Kaneski, C. R., Nagle, J., Bromley, M. C., Colman, M., Schiffmann, R., and Slaugenhaupt, S. A. (2000) *Hum. Mol. Genet.* **9,** 2471–2478
11. Bach, G. (2001) *Mol. Genet. Metab.* **73,** 197–203
12. Altarescu, G., Sun, M., Moore, D. F., Smith, J. A., Wiggs, E. A., Solomon, B. I., Patronas, N. J., Frei, K. P., Gupta, S., Kaneski, C. R., Quarrell, O. W., Slaugenhaupt, S. A., Goldin, E., and Schiffmann, R. (2002) *Neurology* **59,** 306–313
13. Venugopal, B., Browning, M. F., Curcio-Morelli, C., Varro, A., Michaud, N., Nanthakumar, N., Walkley, S. U., Pickel, J., and Slaugenhaupt, S. A. (2007) *Am. J. Hum. Genet.* **81,** 1070–1083
14. Di Palma, F., Belyantseva, I. A., Kim, H. J., Vogt, T. F., Kachar, B., and Noben-Trauth, K. (2002) *Proc. Natl. Acad. Sci. U.S.A.* **99,** 14994–14999
15. Atiba-Davies, M., and Noben-Trauth, K. (2007) *Biochim. Biophys. Acta* **1772,** 1028–1031
16. Grimm, C., Cuajungco, M. P., van Aken, A. F., Schnee, M., Jörs, S., Kros, C. J., Ricci, A. J., and Heller, S. (2007) *Proc. Natl. Acad. Sci. U.S.A.* **104,** 19583–19588
17. Kim, H. J., Li, Q., Tjon-Kon-Sang, S., So, I., Kiselyov, K., and Muallem, S. (2007) *J. Biol. Chem.* **282,** 36138–36142
18. Xu, H., Delling, M., Li, L., Dong, X., and Clapham, D. E. (2007) *Proc. Natl. Acad. Sci. U.S.A.* **104,** 18321–18326
19. Nagata, K., Zheng, L., Madathany, T., Castiglioni, A. J., Bartles, J. R., and García-Añoveros, J. (2008) *Proc. Natl. Acad. Sci. U.S.A.* **105,** 353–358
20. Treusch, S., Knuth, S., Slaugenhaupt, S. A., Goldin, E., Grant, B. D., and Fares, H. (2004) *Proc. Natl. Acad. Sci. U.S.A.* **101,** 4483–4488
21. Venkatachalam, K., Long, A. A., Elsaesser, R., Nikolaeva, D., Broadie, K., and Montell, C. (2008) *Cell* **135,** 838–851
22. Luzio, J. P., Bright, N. A., and Pryor, P. R. (2007) *Biochem. Soc. Trans.* **35,** 1088–1091
23. Luzio, J. P., Pryor, P. R., and Bright, N. A. (2007) *Nat. Rev. Mol. Cell Biol.* **8,** 622–632
24. Kim, H. J., Li, Q., Tjon-Kon-Sang, S., So, I., Kiselyov, K., Soyombo, A. A., and Muallem, S. (2008) *EMBO J.* **27,** 1197–1205
25. Cuajungco, M. P., and Samie, M. A. (2008) *Pflugers Arch.* **457,** 463–473
26. Tieleman, D. P., Shrivastava, I. H., Ulmschneider, M. R., and Sansom, M. S. (2001) *Proteins* **44,** 63–72
27. Dong, X. P., Cheng, X., Mills, E., Delling, M., Wang, F., Kurz, T., and Xu, H. (2008) *Nature* **455,** 992–996
28. Raychowdhury, M. K., González-Perrett, S., Montalbetti, N., Timpanaro, G. A., Chasan, B., Goldmann, W. H., Stahl, S., Cooney, A., Goldin, E., and Cantiello, H. F. (2004) *Hum. Mol. Genet.* **13,** 617–627
29. Kiselyov, K., Chen, J., Rbaibi, Y., Oberdick, D., Tjon-Kon-Sang, S., Shcheynikov, N., Muallem, S., and Soyombo, A. (2005) *J. Biol. Chem.* **280,** 43218–43223
30. Goldin, E., Caruso, R. C., Benko, W., Kaneski, C. R., Stahl, S., and Schiffmann, R. (2008) *Invest. Ophthalmol. Vis. Sci.* **49,** 3134–3142
31. Vergarajauregui, S., Oberdick, R., Kiselyov, K., and Puertollano, R. (2008) *Biochem. J.* **410,** 417–425
32. Soyombo, A. A., Tjon-Kon-Sang, S., Rbaibi, Y., Bashllari, E., Bisceglia, J., Muallem, S., and Kiselyov, K. (2006) *J. Biol. Chem.* **281,** 7294–7301
33. Miedel, M. T., Rbaibi, Y., Guerriero, C. J., Colletti, G., Weixel, K. M., Weisz, O. A., and Kiselyov, K. (2008) *J. Exp. Med.* **205,** 1477–1490
34. Zhang, F., Jin, S., Yi, F., and Li, P. L. (2009) *J. Cell. Mol. Med.*, in press
35. Zhang, F., and Li, P. L. (2007) *J. Biol. Chem.* **282,** 25259–25269
36. LaPlante, J. M., Sun, M., Falardeau, J., Dai, D., Brown, E. M., Slaugenhaupt, S. A., and Vassilev, P. M. (2006) *Mol. Genet. Metab.* **89,** 339–348
37. Reddy, A., Caler, E. V., and Andrews, N. W. (2001) *Cell* **106,** 157–169
38. Cerny, J., Feng, Y., Yu, A., Miyake, K., Borgonovo, B., Klumperman, J., Meldolesi, J., McNeil, P. L., and Kirchhausen, T. (2004) *EMBO Rep.* **5,** 883–888
39. Long, S. B., Campbell, E. B., and Mackinnon, R. (2005) *Science* **309,** 903–908
40. Kress, G. J., Dineley, K. E., and Reynolds, I. J. (2002) *J. Neurosci*. **22,** 5848–5855
41. Xu, H., Jin, J., DeFelice, L. J., Andrews, N. C., and Clapham, D. E. (2004) *PLoS Biol*. **2,** E50
42. Chung, M. K., Güler, A. D., and Caterina, M. J. (2008) *Nat. Neurosci.* **11,** 555–564
43. van Aken, A. F., Atiba-Davies, M., Marcotti, W., Goodyear, R. J., Bryant, J. E., Richardson, G. P., Noben-Trauth, K., and Kros, C. J. (2008) *J. Physiol.* **586**, 5403–5418
44. Jaiswal, J. K., Andrews, N. W., and Simon, S. M. (2002) *J. Cell Biol.* **159,** 625–635
45. Zhang, Z., Chen, G., Zhou, W., Song, A., Xu, T., Luo, Q., Wang, W., Gu, X. S., and Duan, S. (2007) *Nat. Cell Biol.* **9,** 945–953
46. Zhao, Y., Yarov-Yarovoy, V., Scheuer, T., and Catterall, W. A. (2004) *Neuron* **41,** 859–865